A new method of calculation of Franck–Condon factors which includes allowance for anharmonicity and the Duschinsky effect: Simulation of the He I photoelectron spectrum of ClO_2

Daniel K. W. Mok,[a] Edmond P. F. Lee, Foo-Tim Chau,[a] and DeChao Wang
Department of Applied Biology and Chemical Technology, The Polytechnic University of Hong Kong, Hung Hom, Kowloon, Hong Kong

John M. Dyke
Department of Chemistry, University of Southampton, Highfield, Southampton SO17, 1BJ, United Kingdom

(Received 16 May 2000; accepted 10 July 2000)

A new method of Franck–Condon (FC) factor calculation for nonlinear polyatomics, which includes anharmonicity and Duschinsky rotation, is reported. Watson's Hamiltonian is employed in this method with multidimensional *ab initio* potential energy functions. The anharmonic vibrational wave functions are expressed as linear combinations of the products of harmonic oscillator functions. The Duschinsky effect, which arises from the rotation of the normal modes of the two electronic states involved in the electronic transition, is formulated in Cartesian coordinates, as was done previously in an earlier harmonic FC model. This new anharmonic FC method was applied to the simulation of the bands in the He I photoelectron (PE) spectrum of ClO_2. For the first band, the harmonic FC model was shown to be inadequate but the anharmonic FC simulation gave a much-improved agreement with the observed spectrum. The experimentally derived geometry of the $\tilde{X}\,^1A_1$ state of ClO_2^+ was obtained, for the first time, via the iterative FC analysis procedure $\{R(\mathrm{Cl–O})=1.414\pm0.002\,\text{Å}, \angle\mathrm{O–Cl–O}=121.8\pm0.1°\}$. The heavily overlapped second PE band of ClO_2, corresponding to ionization to five cationic states, was simulated using the anharmonic FC code. The main vibrational features observed in the experimental spectrum were adequately accounted for in the simulated spectrum. The spectral simulation reported here supports one of the two sets of published assignments for this band, which was based on multireference configuration interaction (MRCI) calculations. In addition, with the aid of the simulated envelopes, a set of adiabatic (and vertical) ionization energies to all five cationic states involved in this PE band, more reliable than previously reported, has been derived. This led also to a reanalysis of the photoabsorption spectrum of ClO_2. © *2000 American Institute of Physics.* [S0021-9606(00)01337-4]

I. INTRODUCTION

In a recent review on Franck–Condon (FC) analysis and simulation of photoelectron (PE) and electronic bands of small molecules, we have shown that the commonly used harmonic oscillator model might be inadequate in cases where anharmonicity effects are important, such as for vibronic transitions involving vibrational levels of high quantum numbers.[1] The inclusion of anharmonicity into a one-dimensional model (i.e., a single vibrational mode) of Franck–Condon factor (FCF) calculations is relatively straightforward and has been reviewed.[1] However, the applicability of a one-dimensional anharmonic FC model is rather limited. We have suggested, in the above-mentioned review, some possible ways of calculating anharmonic FCFs for vibronic spectra of polyatomics, by employing multidimensional anharmonic potential energy functions (PEFs). In the present work, we report our recently developed, multidimensional anharmonic FCF code for nonlinear polyatomics, which is based on the Watson Hamiltonian[2] and includes the Duschinsky effect.[3] The He I PE spectrum of ClO_2 (Ref. 4) has been chosen for spectral simulation, employing both our previously developed harmonic FCF code CART-FCF[1] and the new anharmonic FCF code AN-FCF. Other than the importance of ClO_2 in atmospheric chemistry (see Sec. I B), one main reason for choosing the PE spectrum of ClO_2 as the first example with which to test the new code is that highly accurate complete active space self-consistent field (CASSCF) MRCI PEFs of the neutral ground state and low-lying cationic states of this intermediate are available.[5,6] Hence, the new anharmonic FCF code can be tested readily, without involving the demanding task of generating high-level *ab initio* PEFs. In the following subsections, we first give a brief review of existing anharmonic FCF calculations before describing the method used in this study.

A. Anharmonic FCF calculations

An anharmonic FCF calculation involves three steps, namely the determination of the multidimensional potential energy surfaces (PEFs) of the two electronic states involved

[a]Authors to whom correspondence should be addressed.

in the electronic transition, the determination of the vibrational wave functions of both electronic states, and the evaluation of the square of the vibrational overlap integrals (i.e., the FCFs). Variational methods have been widely used in determining rovibrational energies of polyatomic molecules. Readers may refer to the two excellent reviews by Carter and Handy[7] and Searles and von Nagy-Felsobuki[8] for details. Also, references which summarize the current status of this area are Refs. 2 and 9–20. To evaluate the FCFs for a polyatomic system, couplings of the vibrational modes (the Duschinsky effect[3]) due to the change in geometry and/or symmetry upon a transition need to be considered;[21] details of this are given in our recent review of polyatomic FCF calculations.[1]

A simple way to include anharmonicity in an FCF calculation is to express the anharmonic vibrational wave functions as linear combinations of the products of harmonic oscillator functions. In this way, the anharmonic vibrational FCF can be reduced to a sum of harmonic overlap integrals, which can be evaluated readily with available analytical formulas. Botschwina and co-workers are one of the few research groups performing anharmonic FCF calculations in this way.[22,23] Recently, details of a few other types of anharmonic FCF methods have been published.[24–28]

The major application of FCF calculations is in spectral simulation. Thus, it is worth mentioning the following recent studies, which are relevant to the present work. Barinovs *et al.*[29] reported the simulation of the absorption spectrum for the $\tilde{A}\,^2A_2 \leftarrow \tilde{X}\,^2B_1$ transition of ClO_2. In their work, 3D wave packet calculations were performed to follow the propagation of the $\tilde{X}\,^2B_1$ ground vibrational wave function onto the $\tilde{A}\,^2A_2$ state PEF. However, it is difficult for this kind of calculation to be extended to molecules with more vibrational modes because of the extensive computational requirements. Last, a novel Lie algebraic formalism has been reported very recently for the evaluation of multidimensional FCFs.[30] In this work, the $\tilde{C}\,^1A\cdot \leftarrow \tilde{X}\,^1A\cdot$ emission spectrum of S_2O was successfully simulated.

B. The He I photoelectron spectrum of ClO_2

Neutral chlorine dioxides have received much attention recently, because of their relevance in the destruction of the ozone layer in the upper atmosphere (see Refs. 1, 4, 5, 6, and 31 and references therein). In contrast, there have been only two experimental studies on the ClO_2 cation in the gas phase. The first He I PE spectrum of ClO_2 was published in 1971.[32,33] Two decades later, Flesch *et al.*[4] reported another He I PE spectrum of ClO_2 with much-improved resolution (quoted to be 15 meV, see the later text). The spectral features in these two PE spectra are very similar in the low ionization energy (IE) region of 10–16 eV, with well-resolved vibrational structure, but differ in the higher IE region, which shows essentially three structureless broad PE bands. Since the later PE spectrum is of a better quality than the one published in 1971, we will focus on the second study from here on and we will only investigate the PE bands observed in the low IE region.

In the low IE region, there are three observed PE bands, which are well separated from each other. The first and third bands, with measured adiabatic ionization energies (AIE) of 10.345 and 15.440 eV, respectively, show clearly resolved vibrational structures, while the second band is a complex one, corresponding to several overlapped ionization structures. Based on consideration of the bonding nature of the high-lying occupied molecular orbitals of neutral ClO_2 (from *ab initio* calculations) and comparison with the known PE spectrum of SO_2, assignments for all the observed bands were made by Flesch *et al.*[4] Ionizations to five cationic states were associated with the second band.[4] In the work of Flesch *et al.*,[4] the photoabsorption spectrum of ClO_2 was also reported and the identified Rydberg series were assigned, with the associated quantum defects (δ) derived, based on the ionization limits measured in the PE spectrum.

It should also be mentioned that Peterson and Werner[5] have reported high-level CASSCF/MRCI calculations (and PEFs; see the next section) on the ground electronic state of ClO_2 and the low-lying states of ClO_2^+. Based on their MRCI results, assignments for the PE spectrum of ClO_2 recorded by Flesch *et al.* were proposed. The assignments of Peterson and Werner[5] differ from those of Flesch *et al.*[4] in the ordering of the five cationic states associated with the second PE band. In the present study, it is hoped that spectral simulations may shed some light on the discrepancies between the two sets of assignments for the heavily overlapped second band in the He I PE spectrum of ClO_2, and may provide vibrational assignments for the first and third bands.

II. THEORY

A. Anharmonic FCF method

The anharmonic FCF method proposed in this investigation is mainly based on that of Botschwina *et al.*[22] One main reason for choosing this approach is that it can be readily incorporated into our existing harmonic FCF model (see the later text). In this way, the Duschinsky effect, which is not considered in the method of Botschwina *et al.*, as mentioned previously, can be included in the present anharmonic FCF method. At the same time, with the use of *ab initio* PEFs and the Cartesian coordinate approach[34–36] (which is good for an electronic transition even with a large geometrical change), many advantageous features of our previous harmonic FCF method are retained (see Ref. 1). Thus, with relatively straightforward modifications to our existing harmonic FCF code, anharmonicity can be incorporated into a multidimensional FCF calculation, which also handles the Duschinsky effect. It is therefore expected that the improved FCF code, which includes anharmonicity, should give more reliable results than the harmonic code. The anharmonic FCF method used in this work will now be described in detail.

The anharmonic FCF method discussed below is based on a nonlinear molecular system, although the method can be easily extended to linear systems. Although the following derivation applies to a molecule with three vibrational modes, the method presented is applicable to problems of any number of modes. First, the anharmonic vibrational wave function of the **m**th vibrational state is expressed as follows:

$$|\mathbf{m}\rangle = \sum c_{\mathbf{m},\mathbf{v}} \phi(v_1)\phi(v_2)\phi(v_3), \quad (1)$$

where $c_{\mathbf{m},\mathbf{v}}$'s are the expansion coefficients, the bold subscript $\mathbf{v}$ denotes (v_1,v_2,v_3) and $\phi(v_i)$ are the vth-order harmonic oscillator functions of the normal mode i. The expansion coefficients, $c_{\mathbf{m},\mathbf{v}}$, are obtained by diagonalizing the Watson's Hamiltonian.[2,9] The rovibrational Hamiltonian of a nonlinear molecule given by Watson has the form

$$H = 1/2\sum_{\alpha\beta} (\Pi_\alpha - \pi_\alpha)\mu_{\alpha\beta}(\Pi_\beta - \pi_\beta) + 1/2\sum_k P_k^2 - 1/8\hbar^2 \sum_\alpha \mu_{\alpha\alpha}^2 + V, \quad (2)$$

where Π is the total angular momentum with respect to the axes of body-fixed coordinates satisfying the Eckart conditions[31] (labeled by the Greek subscripts, $\alpha,\beta,...$), π is the internal angular momentum arising from coupling of vibration modes, P_k is the momentum conjugate to the kth normal coordinate, μ is the effective reciprocal inertia tensor, and V is the electronic PEF. The anharmonicities of the vibrational motions are included in the present formalism via an anharmonic PEF, V, and the anharmonic vibrational wave functions defined in Eq. (1).

The Hamiltonian matrix elements, $\langle \mathbf{n}|H|\mathbf{m}\rangle$, are evaluated using the Gauss–Hermite quadrature along each normal mode. Generally speaking, an *ab initio* PEF will not usually be expressed in normal coordinates. Thus, each quadrature grid point is transformed to the coordinate system of the PEF. Both the vibrational wave functions of the initial and final electronic states are determined in this way. Hence, the anharmonic FCF can be expressed as

$$\mathrm{FCF}(\mathbf{m},\mathbf{n}) = \langle \mathbf{m}|\mathbf{n}\rangle^2 = \left(\sum_{\mathbf{v}',\mathbf{v}''} c_{\mathbf{m},\mathbf{v}'} c_{\mathbf{n},\mathbf{v}''} \langle v_1',v_2',v_3'|v_1'',v_2'',v_3''\rangle \right)^2, \quad (3)$$

where the primed and double-primed quantities correspond to those of the final state and the initial state, respectively. The expansion coefficients $c_{\mathbf{m},\mathbf{v}'}$, and $c_{\mathbf{n},\mathbf{v}''}$ are determined in the variational calculation, and $\langle v_1',v_2',v_3'|v_1'',v_2'',v_3''\rangle$ is the overlap integral of the corresponding harmonic functions. Because the anharmonic wave functions are expressed as linear combinations of harmonic functions in normal coordinates, the overlap integral can be evaluated readily using Chen's model.[37] Also, since the Duschinsky rotation matrix is included in this model, the anharmonic FCFs obtained in this way have incorporated the effect of anharmonicity and Duschinsky rotation.

B. IFCA with the anharmonic FCF method

FCFs are known to be very sensitive to the relative geometries of the electronic states involved in an electronic transition. Thus, if the equilibrium geometry of one of the two electronic states (usually the ground state of the neutral molecule, in the case of a PE spectrum) is available experimentally, the geometry of the other state can be obtained by adjusting its geometrical parameters systematically, until the simulated spectrum matches the experimental spectrum. This iterative Franck–Condon analysis (IFCA) procedure has been applied successfully employing the harmonic FCF code in our previous studies,[38–41] and it has been described previously.[1,37] A similar IFCA procedure can be carried out employing the present anharmonic FCF code. In this case, in the IFCA treatment, the shapes of the *ab initio* PEFs of the two electronic states are kept unchanged. The equilibrium position of one of the two states is fixed to the available experimental geometry, while the geometrical parameters of the other state are varied systematically (initially according to the computed geometry change from *ab initio* calculations), until the best match between the simulated and observed spectra is achieved. More details of the IFCA procedure are given below.

In general, the changes in the geometrical parameters in the IFCA procedure are very small; thus, we would expect the expansion coefficients $c_{\mathbf{m},\mathbf{v}'}$ and $c_{\mathbf{n},\mathbf{v}''}$ obtained at the *ab initio* equilibrium geometries of the PEFs can be kept unchanged in the IFCA procedure. However, the harmonic overlap integrals are very sensitive to the changes in the geometrical parameters. Thus, in the case of an anharmonic FCF calculation, when the geometrical parameters of one state (the cationic state in the case of a PE spectrum) are varied, a new set of harmonic overlap integrals has to be evaluated, which then gives a new set of anharmonic FCFs according to Eq. (3). The simulated spectrum based on this new set of anharmonic FCFs is then compared to the observed spectrum until the best match is obtained.

C. *Ab initio* calculations for the harmonic FCF calculations

Ab initio calculations were performed to provide the harmonic force constants required for the proposed harmonic Franck–Condon analyses and to make comparison with the results of CASSCF/MRCI calculations of Peterson and Werner.[5] In principle, from the available MRCI PEFs,[5] sufficient input data could be obtained for the harmonic FCF calculation. However, in order to compare the harmonic and anharmonic FCF methods in a consistent manner, *ab initio* calculations, which compute harmonic vibrational frequencies at the minimum-energy geometry, were performed, as have been done previously.[1,37] Commonly used single-reference-based correlation methods, such as MP2, QCISD, and coupled-cluster single double (triple) [CCSD(T)] were employed with standard basis sets. Geometry optimization and harmonic vibrational frequency calculations were carried out only for the ground states of the neutral ClO_2 radical, and the ground ($\tilde{X}\,^1A_1$) state and the lowest $^1B_2$ states of the cation, as harmonic FCF calculations were carried out only for the ionization processes to these two ionic states for comparison with the first and third PE bands of ClO_2. All *ab initio* calculations were carried out with the GAUSSIAN98[42] suites of programs.

D. Details of the anharmonic calculations

1. The CASSCF/MRCI PEFs employed

For the anharmonic FCF calculations, the PEFs of the electronic states involved in the electronic transition are required in the variational calculations for the vibrational wave function of each state. For the $\tilde{X}\,^2B_1$ state of ClO_2, the full three-dimensional PEF determined by Peterson[43] was employed. This PEF was obtained by fitting 49 CASSCF/MRCI *ab initio* single-point energies to a polynomial. [Basis sets were employed, which were extended from the standard cc-pVQZ basis sets[44,45] (plus a diffuse *s* and *p* set on both O and Cl, and a tight *d* set on Cl; see Ref. 46).] For the cationic states, the two-dimensional CASSCF/MRCI PEFs of Peterson and Werner[5] were used. [Basis sets of cc-pVQZ (without *g* functions) quality were employed; see Ref. 5 for details.] For each cationic state, the PEF was obtained by fitting 13 computed energy values to a polynomial. These energy points are displacements from the equilibrium position of the symmetry coordinates $S_1=(r_1+r_2)/\sqrt{2}$ and $S_2=\theta$ (see Ref. 5 for details). The above published PEFs were employed in our variational calculations. As the cationic PEFs are two-dimensional, the variational calculations performed are also two-dimensional. The asymmetric stretching mode ν_3 (the third mode) has been neglected in the FCF evaluation. In any case, it is of a different symmetry from the ν_1 and ν_2 modes in the C_{2v} symmetry.

2. The basis size constraints in the variational calculations of the vibrational wave functions

For neutral ClO_2 vibrational levels with quantum number up to 6 were considered in the variational calculations. This should be sufficient, as there is no evidence for ''hot'' bands in the experimental spectrum. To reduce the size of the three-dimensional basis, a further constraint that $v_1+v_2+v_3\leqslant 6$ was applied in the selection of the harmonic basis. For ClO_2^+ vibrational levels with quantum number up to 12 were included, except where stated otherwise. This seemed to be adequate for most cationic states considered here (see the later text). A further constraint of $v_1+v_2\leqslant 12$ was also applied. This constraint (and hence the total size of the basis) was chosen from a series of preliminary calculations on the $\tilde{X}\,^1A_1$ state of ClO_2^+. Variational calculations were performed with the basis set constraints of $v_1+v_2\leqslant 6$, 8, 12, and 20. Results of these calculations are shown in Table I. Only the energies of the progression in the stretching mode are given as the experimental spectrum is dominated by this progression. With the basis set constraint of up to $v_1+v_2\leqslant 12$, the computed vibrational energies of the levels (0,0,0) to (5,0,0) converge to within 1 cm^{-1} of the $v_1+v_2\leqslant 20$ values, while for the vibrational level (6,0,0), the computed energy converges to within 6 cm^{-1}. It seems that the basis set constraint of $v_1+v_2\leqslant 12$ is a reasonable compromise of accuracy and economy, at least for the $\tilde{X}\,^1A_1$ state of ClO_2^+. This constraint has been applied for most of the cationic states considered here, unless otherwise stated.

Since the FCFs depend on the expansion coefficients $c_{\mathbf{m},\mathbf{v}'}$, the convergent behavior of these coefficients with the size of the basis set used was studied. It was found that the convergent behavior of the expansion coefficients generally follows that of the computed vibrational energies. The differences between the calculated vibrational energies obtained with the two basis set constraints of $v_1+v_2\leqslant 12$ and 20 for the levels (5,0,0) and (6,0,0) of the $\tilde{X}\,^1A_1$ state of ClO_2^+ are 0.5 and 5.4 cm^{-1}, respectively. The corresponding differences in the three largest expansion coefficients are less than 0.001 and 0.01, respectively. For vibrational levels $(v,0,0)$ with $v<4$, the differences in the expansion coefficients determined using basis set constraints of $v_1+v_2\leqslant 12$ and 20 are smaller than 0.000 01.

TABLE I. Computed vibrational energies (with respect to the ground vibrational state in cm^{-1}) using the ClO_2^+ $X\,^1A_1$ potential surface of Peterson and Wernet (Ref. 5) with different basis set sizes.

Constraints	$v_1+v_2=6$	$v_1+v_2=8$	$v_1+v_2=12$	$v_1+v_2=20$
Zero point energy	1398.9	1398.9	1398.9	1398.9
(1,0,0)	997.8	997.8	997.8	997.8
(2,0,0)	1985.0	1984.8	1984.8	1984.8
(3,0,0)	2968.2	2962.0	2961.6	2961.6
(4,0,0)	3972.3	3933.4	3929.0	3929.0
(5,0,0)	5022.0	4930.1	4888.2	4887.7
(6,0,0)	6739.0	5978.0	5844.0	5838.6
Basis set size	28	45	153	231

To further examine the effect of basis set size in the calculation of vibrational wave functions on the computed anharmonic FCFs, the FCFs between the $\tilde{X}$ states of ClO_2 (0,0,0) and ClO_2^+ $(v,0,0)$ were calculated, employing the basis set constraints of $v_1+v_2\leqslant 12$ and 20 for the upper vibrational states. With the larger constraint, the anharmonic FCFs for the (4,0,0), (5,0,0), and (6,0,0) levels of ClO_2^+ from the $\tilde{X}$ state (0,0,0) level of ClO_2 have the values of 1.4208, 0.0919, and 0.0028, respectively (with the FCF of the strongest peak taken as 100). With the smaller basis set constraint of $v_1+v_2\leqslant 12$, the corresponding computed anharmonic FCFs differ from those computed with the larger basis set constraint of $v_1+v_2\leqslant 20$ by 0.007%, 0.2%, and 3.5%, respectively. For the (6,0,0) vibrational component, which has the largest deviation in the computed FCFs with the two basis set constraints used, it is too weak to be observed in the experimental spectrum. Summing up the above investigations on the effects of the basis set size employed in the variational calculation of vibrational wave functions, on the computed vibrational energies expansion coefficients and FCFs, it is concluded that the basis set constraint of $v_1+v_2\leqslant 12$ for the upper vibrational states should be acceptable. The uncertainty in the simulated intensities obtained with this constraint should be less than 1%.

3. The performance of the anharmonic FCF code

The variational calculations and the evaluation of anharmonic FCFs were performed using the software AN-FCF coded in FORTRAN. The largest variational calculation shown in Table I required 69 s CPU time on a Pentium II 300 PC with 128 MB of physical memory. The computational time of the calculation increases tremendously with the size of the basis set, especially in the evaluation of the FCFs. For the

TABLE II. The computed optimized geometries and harmonic vibrational frequencies (cm^{-1}) of the $\tilde{X}\,^2B_1$ state of OClO.

Method	r_e/Å	θ/°	$\omega_1(a_1)$	$\omega_2(a_1)$	$\omega_3(b_2)$	Reference
UMP2/6-311G(2*d*)	1.4976	119.09	966.3	431.0	1124.9	This work
UMP2/6-311G(3*df*)	1.4694	118.08	1037.6	452.2	3083.7	This work
UQCISD/6-311G(2*d*)	1.4968	117.62	904.9	435.8	1073.1	This work
UQCISD/6-311G(3*df*)	1.4653	116.90	a			This work
UCCSD(T)/6-311G(3*df*)	1.4760	117.46	a			This work
CASSCF/MRCI/ cc-pVQZ (no *g*)	1.480	117.8	945	452		5
CASSCF/MRCI+*Q*/ cc-pVQZ (no *g*)	1.488	117.4	928	442		5
CASSCF/MRCI+*Q*/ cc-pVQZ	1.4728	117.65	960.2	455.6	1127.9	43
Expt.	1.4698	117.41	963.5	451.7	1133.0	46,47

[a]SCF convergence problems in the numerical second derivative calculations.

second band in the ClO_2 photoelectron spectrum, a larger basis set size was required for the $^3A_1$ and the $^1A_1$ states as the computed FCFs suggest significant relative intensities for peaks of higher vibrational quantum numbers than 12 (see the next section). For these two states, the variational calculations had a basis set size of (12,18,0) with a constraint of $v_1+v_2\leqslant 18$, and the largest FCF evaluations carried out in this work for ionization to these two cationic states involved 84 and 221 vibrational levels for the initial and the final electronic states, respectively. These FCF calculations took ca. half an hour CPU time (per cationic state) with the above-mentioned PC. After evaluating the FCFs, Gaussian functions with a full-width-half-maximum (FWHM, see the next section) of 30 meV and relative intensities as given by the corresponding FCFs were used to simulate the vibronic peaks.

III. RESULTS AND DISCUSSION

A. *Ab initio* calculations

The *ab initio* results obtained in this work for ClO_2 $\tilde{X}\,^2B_1$, ClO_2^+ $\tilde{X}\,^1A_1$, and ClO_2^+ $^1B_2$ are summarized in Tables II–V and compared with available experimental values and previous theoretical values. Briefly, it can be seen that for the three electronic states studied, no obvious trends in the computed geometrical parameters and harmonic vibrational frequencies are observed with the theoretical method used. This shows the difficulty in achieving convergence in the calculated parameters for this type of system. Nevertheless, for the ground states of the neutral and the cation, the computed bond angles at different levels of calculation are reasonably consistent. Therefore, they can be considered as reliable. However, for the open-shell $^1B_2$ state the UHF-based correlation methods used in this study are clearly inadequate for the minimum-energy geometry, particularly for the computed bond angles, which have a range of ca, 10°. Regarding the computed harmonic vibrational frequencies, the QCISD values are the nearest to the available experimental values, and hence the corresponding force constants were used in the subsequent Franck–Condon calculations.

Considering the computed AIEs and VIEs (see Table V), for the ionization to the ground state of the cation, the CCSD(T)/cc-pVQZ values agree very well with the experimental values. This excellent agreement of within ca. 0.05 eV is even better than that of the MRCI results from Peterson and Werner.[5] From Table V, it is clear that basis size effect is important for the calculation of reliable AIE/VIE values for this type of system. Other than the size-inconsistency

TABLE III. The computed optimized geometries and harmonic vibrational frequencies (cm^{-1}) of the $\tilde{X}\,^1A_1$ state of $OClO^+$.

Method	r_e/Å	θ/°	$\omega_1(a_1)$	$\omega_2(a_1)$	$\omega_3(b_2)$	Reference
MP2/6-311G(2*d*)	1.4609	123.00	923.1	457.4	1189.6	This work
MP2/6-311G(3*df*)	1.4313	122.88	1006.9	477.8	1275.1	This work
QCISD/6-311G(2*d*)	1.4265	121.02	1019.2	503.6	1210.1	This work
QCISD/6-311G(3*df*)	1.4014	121.30	1127.5	527.6	1409.1	This work
CCSD(T)/6-311G(3*df*)	1.4176	121.50	1047.5	498.5	1330.5	This work
QCISD/6-311+G(2*d*)	1.428	121.0	1012	500	1280	48
CASSCF/MRCI/ cc-pVQZ (no *g*)	1.423	120.78	1012	511		5
CASSCF/MRCI+*Q*/ cc-pVQZ (no *g*)	1.431	120.6	988	497		5
CCSD(T)/cc-pVQZ	1.4252	120.81	1027.8	502.7	1300.9	49
IFCA (harmonic)	1.410	121.8				This work
IFCA (anharmonic)	1.414	121.8				This work
Expt.			1020±20	520±20		50

TABLE IV. The computed optimized geometries and harmonic vibrational frequencies (cm^{-1}) of the $^1B_2$ state of $OClO^+$.

Method	r_e/Å	θ_e/°	$\omega_1(a_1)$	$\omega_2(a_1)$	$\omega_3(b_2)$	Reference
CIS/6-311G(2*d*)	1.4835	110.86	1034.6	368.8	470.2	This work
UMP2/6-311G(2*d*)	1.5405	119.53	1232.1	365.9	1058.3	This work
UMP2/6-311G(3*df*)	1.5260	118.99	1189.8	351.8	913.7	This work
UQCISD/6-311G(2*d*)	1.5991	107.78	690.8	322.6	416.7	This work
UQCISD/6-311G(3*df*)	1.5511	107.14	801.6	377.8	563.8	This work
UCCSD(T)/6-311G(3*df*)	1.5954	108.22	a			This work
CASSCF/MRCI/ cc-pVQZ (no *g*)	1.5619	113.58	775	225		5
CASSCF/MRCI+*Q*/ cc-pVQZ (no *g*)	1.577	113.3	725	216		5
IFCA (harmonic)	1.558	114.5				This work
IFCA (best estimate)[b]	1.56	114.0				This work
Expt.			766			4,51

[a]SCF convergence problems in the numerical second derivative calculations.
[b]The best estimate geometry from anharmonic IFCA; please refer to the discussion in the text.

problem with the MRCI method, the omission of *g* functions in the cc-pVQZ basis set in the MRCI calculations of Peterson and Werner may be a reason for the relatively large discrepancies of more than 0.3 eV between the MRCI AIE/VIE and the experimental values. However, for the ionization to the $^1B_2$ state, the UHF-based correlation methods employed here are, again, clearly inadequate (see Ref. 39 for a similar conclusion), as shown from the large discrepancies between their computed AIEs and the CASSCF/MRCI and experimental values.

B. Spectral simulation: First PE band

The simulations of the first band in the PE spectrum of ClO_2, employing the harmonic and anharmonic FCF codes, are shown in Figs. 1(c) and 1(b), respectively, together with the experimental spectrum of Flesch *et al.*[4] [Fig. 1(a)]. This band is due to the ClO_2^+ $\tilde{X}\,^1A_1 \leftarrow ClO_2$ $\tilde{X}\,^2B_1$ ionization and has the most clearly resolved vibrational structure. The experimental spectrum is dominated by the symmetric stretching progression. Although structure in the bending progression is relatively weak, the resolution is good enough to reveal the bending features. Thus, the observed vibrational structure provides sufficient information for both the bond angle and the bond length of the ground cationic state to be extracted from comparison between the simulated and observed spectra via the IFCA procedure. The details of the comparison are given in the following subsections for the harmonic and anharmonic FC simulations.

1. Harmonic FC simulation

The simulated first band [Fig. 1(c)] with harmonic FCFs was obtained with the experimental AIE[4] and the experimental geometry of the $\tilde{X}\,^2B_1$ state.[46,47] The QCISD/6-311G(2*d*) and QCISD/6-311G(3*df*) harmonic force constants were used for the neutral and the cationic ground states, respectively, in the FCF calculations. The IFCA procedure has been applied and the geometry, $R(\mathrm{Cl–O})=1.410\pm0.010$ Å, $\angle\mathrm{O–Cl–O}=121.8\pm0.5°$, is found to give the ''best'' match between the simulated and observed spectra. This simulated spectrum is shown in Fig. 1(c). However, it can be seen from Figs. 1(c) and 1(a) that the match is far from perfect. Despite various attempts, it was not possible to match the component relative intensities across the whole stretching progression within the whole PE band. The above IFCA geometry was obtained by matching the relative intensities of the first three most intense components, where the anharmonic effect

TABLE V. The computed AIEs (VIEs) (in eV) for the first ($\tilde{X}\,^1A_1$ $OClO^+$) and third bands ($^1B_2$ $OClO^+$) in the He I PE spectrum of OClO.

Method	$\tilde{X}\,^1A_1$	$^1B_2$	Reference
UMP2/6-311G(2*d*)	9.68	15.52	This work
UMP2/6-311G(3*df*)	9.80	15.72	This work
UQCISD/6-311G(2*d*)	10.15	12.82	This work
UQCISD/6-311G(3*df*)	10.20	13.32	This work
UCCSD(T)/6-311G(3*df*)	10.04	12.37	This work
PMP2/cc-pVQZ//UCCSD(T)/6-311G(3*df*)	10.07	15.76	This work
PMP3/cc-pVQZ//UCCSD(T)/6-311G(3*df*)	10.67	16.68	This work
MP4SDQ/cc-pVQZ//UCCSD(T)/6-311G(3*df*)	10.40	13.75	This work
UCCSD/cc-pVQZ//UCCSD(T)/6-311G(3*df*)	10.50;[10.78]	13.73	This work
UCCSD(T)/cc-pVQZ//UCCSD(T)/6-311G(3*df*)	10.30;[10.42]	12.57	This work
CASSCF/MRCI/cc-pVQZ	9.72;[9.86]	14.87;[15.12]	5
CASSCF/MRCI+Q/cc-pVQZ	10.06;[10.11]	14.92;[15.25]	5
Expt.	10.345;[10.475]	15.250;[15.440]	4,51

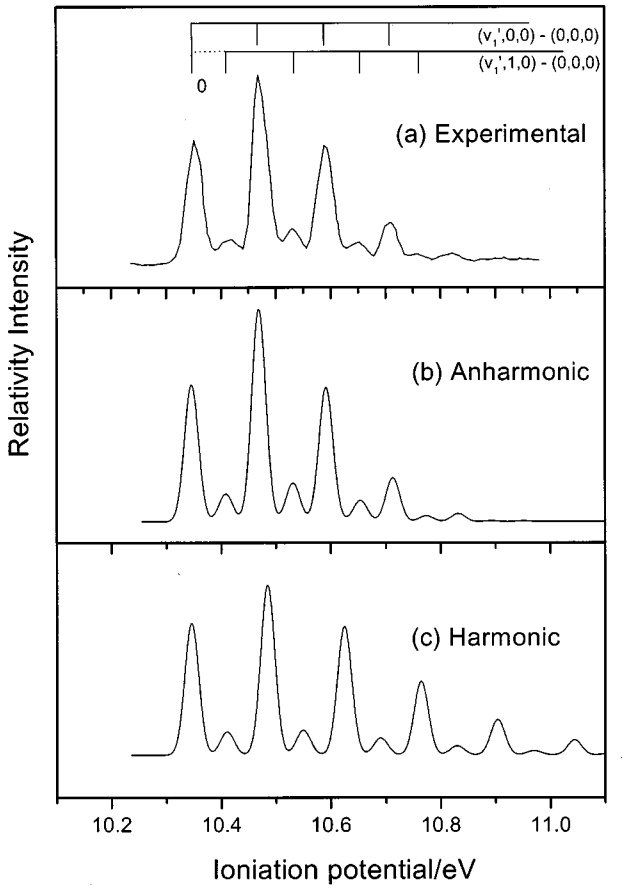

FIG. 1. The first band of the ClO_2 photoelectron spectrum: (a) the experimental spectrum (Ref. 4), (b) the simulated spectrum obtained using anharmonic FCFs, and (c) the simulated spectrum using harmonic FCFs.

would be expected to be the least important (see Ref. 1). With this IFCA geometry, simulated components involving higher stretching levels are significantly stronger than the observed ones, suggesting that the harmonic oscillator model is probably inadequate. Apart from the stretching progression, the first bending peak (0,1,0) is too strong in the simulation. From the comparison between the anharmonic FC simulation and the observed first band (see the next subsection), it seems clear that both the symmetric stretching and bending modes are significantly anharmonic in the ground cationic state of ClO_2^+. Consequently, the simulated spectrum using the harmonic FCFs failed to reproduce the overall intensity pattern of the two progressions observed in He I PE spectrum. In view of this inadequacy, rather large uncertainties have been included for the geometrical parameters given above. From the harmonic calculation, it was found that the FCFs for transitions involving the asymmetric stretching mode, ν_3, are negligible. This shows that the neglect of the asymmetric stretching mode in the anharmonic FCF calculation is a good approximation and should have little impact on the accuracy of the spectral simulation.

2. Anharmonic FC simulation

The expansion coefficients $c_{\mathbf{m},\mathbf{v}'}$ obtained from the variational calculation are an indication of the degree of anharmonicity with the chosen PEF. The first three terms in the first five anharmonic vibrational wave functions of the ground state of ClO_2^+ with a basis set of $v_1+v_2\leqslant 12$ are given below

$$
\begin{aligned}
|0,0,0\rangle &= 0.998\phi(0,0,0) - 0.056\phi(0,0,0) \\
&\quad - 0.015\phi(0,0,0) + \cdots, \\
|0,1,0\rangle &= 0.997\phi(0,1,0) - 0.059\phi(1,1,0) \\
&\quad + 0.040\phi(0,2,0) + \cdots, \\
|1,0,0\rangle &= 0.974\phi(1,0,0) - 0.154\phi(0,2,0) \\
&\quad - 0.151\phi(2,0,0) + \cdots, \\
|0,2,0\rangle &= 0.982\phi(0,2,0) + 0.153\phi(1,0,0) \\
&\quad - 0.073\phi(0,3,0) + \cdots, \\
|2,0,0\rangle &= 0.927\phi(2,0,0) - 0.264\phi(3,0,0) \\
&\quad - 0.192\phi(1,2,0) + \cdots,
\end{aligned}
\tag{4}
$$

where $\phi(v_1,v_2,v_3)$ stands for harmonic basis function $\phi(v_1)\phi(v_2)\phi(v_3)$. The deviation of the leading coefficient from unity shows the deviation from the dominant harmonic function, and is thus a measure of anharmonicity. From the above, the $|0,0,0\rangle$ and $|0,1,0\rangle$ states are very close to the case of a harmonic oscillator, as expected. Higher vibrational states are more and more anharmonic. In addition, the stretching progression seems to be more anharmonic than the bending progression.

From Fig. 1, it is clear that anharmonic FCF calculations have produced a much better simulated spectrum than the harmonic FCF calculations, when compared with the observed spectrum. The IFCA procedure, as described in the previous section, has been carried out to obtain the derived IFCA geometry for the ground cationic state, which gave the best simulated spectrum, as shown in Fig. 1(b). The match between the anharmonic simulated and observed spectra is excellent. The IFCA geometry of the cation is $R(\mathrm{Cl–O})=1.414\pm0.002$ Å and $\angle\mathrm{O–Cl–O}=121.8\pm0.1°$. It is of interest to note that the anharmonic IFCA geometry is close to that of the harmonic IFCA one.

C. Spectral simulation: Third PE band

The simulated third band using both the harmonic and anharmonic FCFs is shown in Fig. 2. The third band of the ClO_2 PE spectrum is essentially a progression in the symmetric stretching mode. Although no expanded spectrum of the third band is given in Ref. 4, at least seven components can be identified for this progression. Cornford *et al.*[33] reported a measured bending frequency of 440 cm^{-1} in the third PE band of ClO_2. However, no bending vibrational frequency was reported in Ref. 4 for this band. Although *ab initio* calculations have not given a consistent value of the bending frequency for the $^1B_2$ state of ClO_2 (see Table IV), all the computed values are significantly smaller than the reported value of Cornford *et al.* In view of the superior quality of the observed spectrum of Ref. 4, it seems that the reliability of the bending frequency reported by Cornford *et al.* is doubtful.

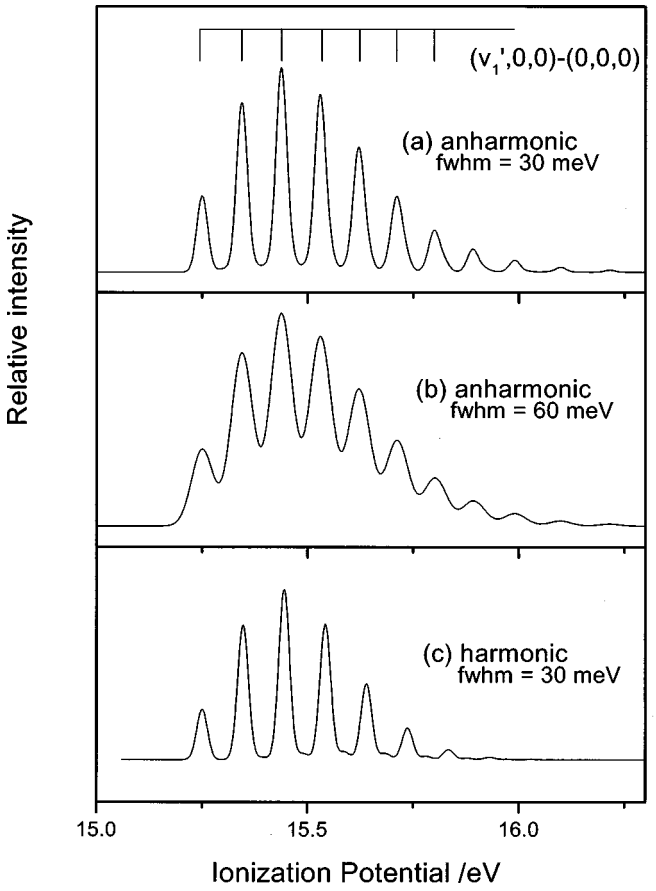

FIG. 2. The third band of the ClO_2 photoelectron spectrum: (a) the simulated spectrum using anharmonic FCFs, (b) same as above, but with a FWHM of 60 meV, and (c) the harmonic simulated spectrum.

The harmonic FC simulation shown in Fig. 2(c) was obtained with an IFCA geometry of $R(\mathrm{Cl–O})=1.558$ Å and $\angle \mathrm{O–Cl–O}=114.5°$. The match between the simulated and observed spectra is mainly based on the first three vibrational components, and assuming that the relative intensities of bending mode components are negligibly small. The IFCA procedure has not been performed for this PE band with the anharmonic simulation, because the match between the anharmonic FC simulated spectrum, obtained with the MRCI geometries, and the observed spectrum is already satisfactory. This suggests that the computed MRCI geometry change upon ionization to the $^1B_2$ state is probably reliable. Considering both the IFCA results with the harmonic simulation discussed, and the good agreement between the MRCI anharmonic simulation with the observed spectrum, the best estimate of the geometry for the $^1B_2$ state from the present study is $R(\mathrm{Cl–O})=1.56\pm0.01$ Å and $\angle \mathrm{O–Cl–O}=114.0\pm1.0°$. The large uncertainties associated with the estimated values of these geometrical parameters are mainly due to the relatively poorer quality of the observed third PE band.

The major difference between the anharmonic and harmonic FC simulations of the third PE band [Figs. 2(a) and 2(c)] is that the former gives a longer stretching progression. Comparison between the simulated and experimental spectra suggests that the anharmonic simulation appears to be in slightly better agreement with experiment. In Figs. 2(a) and 2(c), a FWHM of 30 meV has been used. This value was obtained by measuring the FWHM of a vibrational component in the first band given in Ref. 4, and is significantly larger than the quoted resolution of 15 meV. The observed third band[4] appears to be of even poorer resolution. Hence, a simulated spectrum with a FWHM of 60 meV is also given [Fig. 2(b)] for comparison.

D. Spectral simulation: Second PE band

Based on the MRCI calculations of Peterson and Werner,[5] the second PE band of ClO_2 consists of ionizations to five electronic states of ClO_2^+, namely the $^3A_1$, $^3B_1$, $^3B_2$, $^1A_1$, and $^1B_2$ states. Both Flesch *et al.*[4] and Peterson and Werner[5] assigned these five cationic states to the second PE band of ClO_2, but the assignments of the relative energy ordering of these states and hence their adiabatic ionization energies (AIEs) are different. The two sets of assignments are showed in Table VI. In order to confirm or revise these assignments, in particular, the relative energy ordering of these five cationic states, the ionizations to these five cationic states were simulated, employing the anharmonic FCF code with the MRCI PEFs of Peterson and Werner.[5] The simulated spectra are shown in Figs. 3–5. The profiles of these simulated spectra are quite different, and it will be seen that they are very useful in clarifying the ionic state ordering, which is discussed in the following section.

TABLE VI. The AIEs (VIE) of the five cationic states in the second PE band of ClO_2 according to the assignments of Flesch *et al.* (Ref. 4), Peterson and Werner (Ref. 5), and the anharmonic FC simulations from this work (see the text).

AIE (VIE)/eV	Flesch *et al.* (Ref. 4)	Peterson and Werner[a] (Ref. 5)	Anharmonic FC simulation
$^3B_2$	12.870 (12.990)	12.29 (12.7)	12.400 (12.693)
$^3A_2$	13.330 (13.330)	12.46 (12.8)	12.570 (13.040)
$^3B_1$	12.400 (12.590)	12.78 (13.0)	12.785 (12.872)
$^1A_2$	13.500 (13.590)	12.78 (13.1)	12.890 (13.386)
$^1B_1$	12.455 (12.635)	13.22 (13.6)	13.330 (13.579)

[a]The AIEs are the MRCI+Q/cc-pVQZ (with 1g) energies of the corresponding cationic states relative to the $\tilde{X}\,^1A_1$ state of ClO_2^+, plus the experimental AIE (10.350 eV) of the $\tilde{X}\,^1A_1$ state; the VIEs are the MRCI+Q/cc-pVQZ (with 1g) values shifted by 0.37 eV to approximate the match of the computed and observed first AIE.

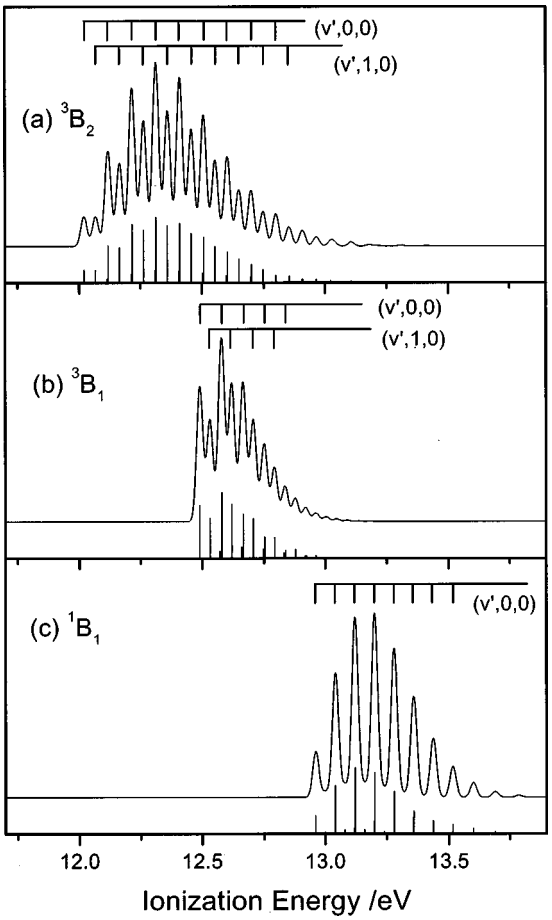

FIG. 3. The simulated photoelectron spectra for the ionization from ground state of ClO_2 to: (a) the $^3B_2$ state of ClO_2^+, (b) the $^3B_1$ state of ClO_2^+, and (c) the $^1B_1$ state of ClO_2^+ (see the text for further details).

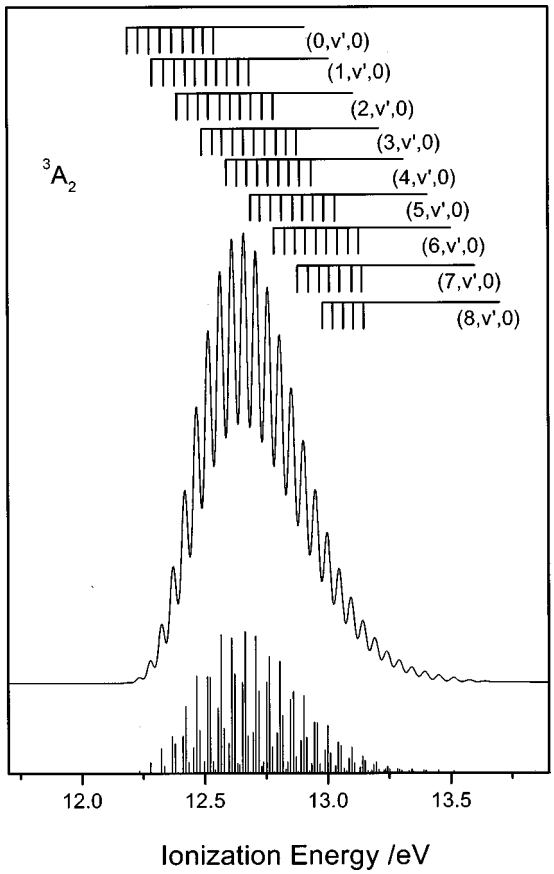

FIG. 4. The simulated photoelectron spectrum of the ClO_2^+ $^3A_2 \leftarrow ClO_2$ $\tilde{X}\,^2B_1$ ionization (see the text for further details).

1. New assignments based on comparison between simulated and observed vibrational structures

For convenience of discussion, the second band has been partitioned into three regions, the low-energy, mid-energy, and high-energy region. The low-energy region covers 12.4 eV to about 12.8 eV, which exhibits resolved vibrational structure; there are essentially five pairs of peaks. A more careful inspection of the vibrational structure through this region suggests that the first pair through the fourth pair appear to be from the same ionization process, with a gradual increase and then decrease in their relative intensities. The fifth pair of peaks seems stronger than the fourth pair, suggesting that another ionization starts from here and extends into the mid-energy region. The mid-energy region has the range of 12.9 to 13.2 eV. In this region, four or five peaks appear to be from the same vibrational progression. The high-energy region is from 13.2 eV onward and the vibrational structure is less obvious here.

We first consider the low-energy region, where the well-resolved vibrational structure is observed. The simulated $ClO_2^+\,^3B_1 \leftarrow ClO_2\tilde{X}\,^2B_1$ and $ClO_2^+\,^3B_2 \leftarrow \tilde{X}\,^2B_1$ bands [Figs. 3(b) and 3(a), respectively] are both dominated by the stretching $(v,0,0)$ and the combination bands $(v,1,0)$, giving two vibrational progressions. They clearly resemble the vibrational structure observed in the low-energy region of the second band with five ''pairs'' of peaks. Flesch *et al.*[4] assigned these two progressions (pairs of peaks) to the ionizations to the $^{3,1}B_1$ electronic states (i.e., two nearby cationic states, each with a single vibrational progression, instead of two vibrational progressions of the same electronic state). However, both the computed MRCI triplet/singlet splitting (and/or the AIEs, see Table VI) and our simulations of these two ionizations [Figs. 3(b) and 3(c)] do not support the assignments of Flesch *et al.*[4] (The assignments of Peterson and Werner[5] will be considered later.)

Based on the simulated spectra, the low-energy region of the second PE band is now reassigned to the ionizations to the $^3B_2$ and $^3B_1$ states, with the pairwise structures assigned to the symmetric stretch and bending modes. The $^3B_1$ simulation [Fig. 3(b)] shows a sharp adiabatic peak in the vibrational structure, while the relative intensities of the two vibrational progressions of the $^3B_2$ simulation [Fig. 3(a)] increase gradually. These simulated vibrational envelopes support the assignments that the observed onset of the second PE band at 12.400 eV is the AIE position of the $^3B_2$ state. The MRCI calculations[5] also give the $^3B_2$ state as the lowest state of the five cationic states assigned to the second PE band. The AIE position of the ionization to the $^3B_1$ state is then assigned to the fifth pair of vibrational components in the low-energy region measured at 12.785 eV. These assignments give a relative energy (T_0) between the $^3B_2$ and $^3B_1$ state of 0.385 eV, which compares reasonably well with the

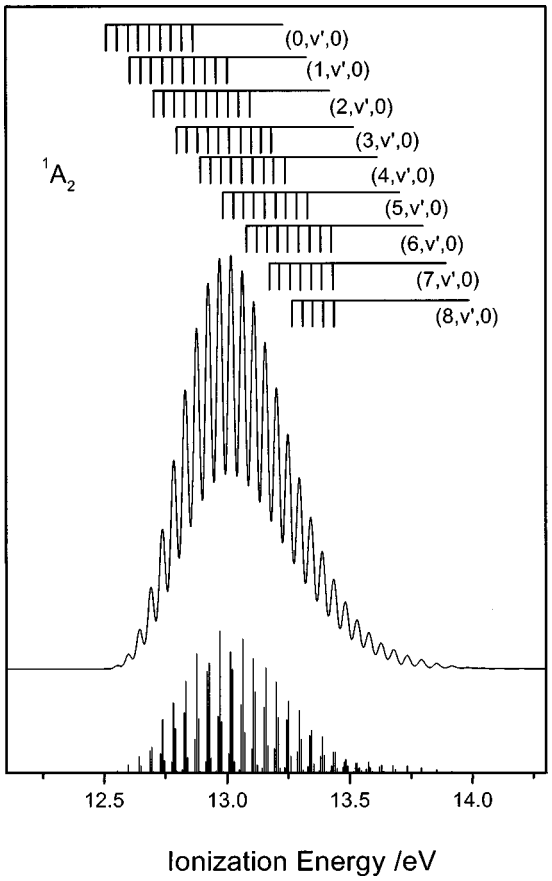

FIG. 5. The simulated photoelectron spectrum of the ClO_2^+ $^3A_1 \leftarrow ClO_2$ $\tilde{X}\,^2B_1$ ionization (see the text for further details).

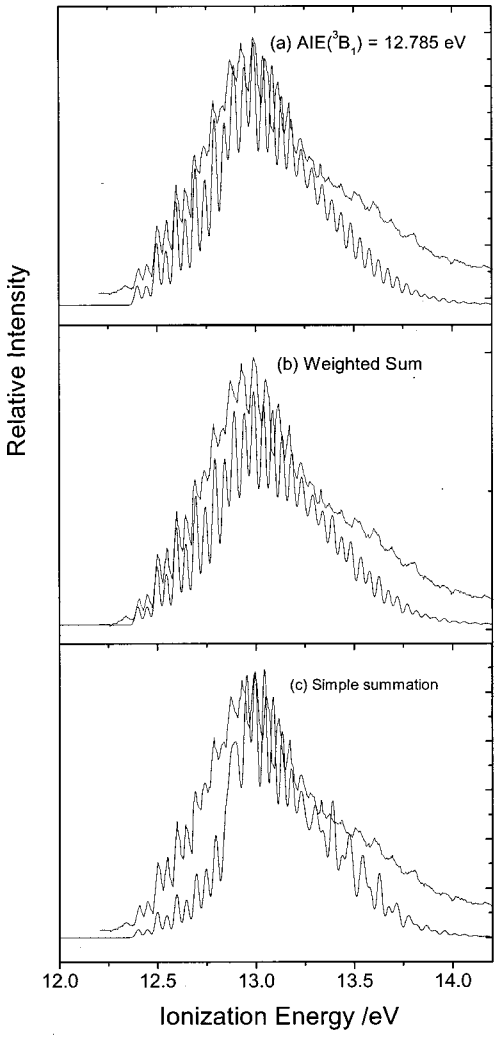

FIG. 6. The synthesized second band of the ClO_2 photoelectron spectrum (lower trace) and the experimental spectrum (upper trace) of Flesch *et al.* (Ref. 4) (see the text for details): (a), the best match, as (c) and (b), but with AIE ($^3B_1$) set to 12.785 eV; (b), as (c) but with adjusted relative photoionization cross sections (see the text); (c) with MRCI+Q AIEs+0.38 eV shift.

MRCI+Q/cc-pVQZ (with g) relative T_e value of 0.47 eV.

From the MRCI calculations, the AIE to the $^3A_2$ state was computed to be in between those of the $^3B_2$ and $^3B_1$ state. However, our simulation of the ClO_2^+ $^3A_2$ $\leftarrow ClO_2$ $\tilde{X}\,^2B_1$ ionization (Fig. 4) shows long progressions in the symmetric bending and stretching vibrations, suggesting a very weak relative intensity at the adiabatic position of the $^3A_2$ ionization, which would probably be too weak to be identified in the observed spectrum. Nevertheless, if the vertical ionization position (strongest overall relative intensity) of the simulated spectrum is aligned to the observed peak at 13.050 eV (having the strongest resolved relative peak intensity) in the mid-energy region, an AIE of 12.580 eV can be obtained from the simulation. This AIE value corresponds very well with the MRCI value of 12.46 eV (see Table VI). This assignment of the $^3A_2$ state would then account for the observed single progression in the mid-energy region.

Before the whole second PE band is considered, we look briefly at the simulated envelopes for ionization to the two singlet states. The simulations for the $^1A_2$ and $^1B_1$ states are shown in Figs. 5 and 3(b), respectively. These singlet states are expected to be weaker than their corresponding triplet states (with a statistical ratio of 1:3). The vibrational structure of the $^1A_2$ band is very similar to the triplet counterpart (Figs. 4 and 5), but the $^1B_1$ simulated spectrum, dominated by the stretching $(v,0,0)$ progression, is quite different from that of the $^3B_1$ band. The latter difference is not surprising, as the triplet and singlet states have considerably different bond angles (from the MRCI calculations[5]).

2. The simulation of the second PE band

Considering the assignments of Peterson and Werner,[5] which were mainly based on computed MRCI AIEs/VIEs, the whole second band of the ClO_2 PE spectrum was synthesized by a weighted sum of the five constituent simulated spectra. The MRCI+Q AIEs, shifted by 0.38 eV in order to match approximately the observed values, were used. Thus, for ionization to the $^3B_2$, $^3A_2$, $^3B_1$, $^1A_2$, and $^1B_1$ states from ClO_2 $\tilde{X}\,^2B_1$, the AIEs after the shift are 12.40, 12.57, 12.87, 12.89, and 13.33 eV, respectively. In Fig. 6(c), the simulated spectrum (lower trace) was generated by simple addition of the five simulated spectra, assuming the same photoionization cross section for each ionization, but with allowance for the statistical weights of spin multiplicity. That is, the total relative intensities between the $^3A_2$ and $^1A_2$ spectra and that of the $^3B_1$ and $^1B_1$ spectra were assumed to be 3 to 1, while ionization to the three triplet states was assumed

TABLE VII. Revised quantum defects (δ) of the Rydberg series observed in the photabsorption spectrum of ClO_2 by Flesch *et al.* (Ref. 4), based on the new AIE positions obtained in this work.

E_R(eV) Origin	$^3B_2$ AIE=12.400 eV		$^3A_2$ AIE=12.570 eV		$^3B_1$ AIE=12.785 eV	
	nl	δ	nl	δ	nl	δ
9.117			$4s$	2.02	$4s(\nu_1)$	1.93
9.161					$4s(\nu_2)$	
9.838	$4p(\nu_1)$	1.70	$4p$	1.77	$4p(\nu_1)$	1.85
9.894	$4p(\nu_2)$				$4p(\nu_2)$	
9.922	$4p'(\nu_1)$	1.66	$4p'$	1.73	$4p'(\nu_1)$	1.82
9.970	$4p'(\nu_2)$				$4p'(\nu_2)$	
10.138					$4p''(\nu_1)$	1.73
10.184					$4p''(\nu_2)$	
11.191	$5p(\nu_1)$	1.65				
11.242	$5p(\nu_2)$					
11.286			$5p$	1.75	$5s$	1.99
11.606					$5p$	1.60
11.649	$6p(\nu_1)$	1.75	$6s$	2.16		
11.693	$6p(\nu_2)$					
12.195			$8s$	1.98	$7s$	2.20

to have the same intensity. The agreement between the spectrum synthesized in this way [the lower trace in Fig. 6(c)] and the experimental spectrum [the upper trace in Fig. 6(c)] is reasonably good, particularly for the resolved vibrational structure. In general, most of the observed vibrational features can be accounted for by the simulations, suggesting that the assignments of Peterson and Werner[5] are reasonably reliable.

A better agreement between the simulated second band and the observed one can be obtained by varying the relative intensities between the $^3B_2$, the $^3A_2$ and $^1A_2$ pair, and the $^3B_1$ and $^1B_1$ pair, and also the AIEs. Figure 6(c) shows the best matching spectrum (lower trace) obtained by varying the relative intensities. The relative intensities for the $^3B_2$, $^3A_2$, and $^3B_1$ ionizations used are 3, 0.3, and 1.5, respectively (assuming a triplet to singlet statistical ratio of 3:1). Efforts were also made to improve the agreement by changing the AIE of each ionization. From the previous subsection, we have assigned the 12.785 eV peak to the AIE of the $^3B_1$ ionization. The simulated second PE band employing this AIE for the $^3B_1$ ionization is shown in Fig. 6(a). In the low- and mid-energy region, this simulation seems to be in marginally better agreement with the experimental band than the one using the shifted MRCI+Q AIEs. Further attempts were made in varying each AIE of the individual ionizations in order to obtain a better match with the experimental band. However, no further improvement could be achieved and the synthesized second PE band shown in Fig. 6(a) is the best match that can be obtained. Thus, the best AIEs to the $^3B_2$, $^3A_2$, $^3B_1$, $^1A_2$, and $^1B_1$ states are estimated to be 12.400, 12.570, 12.785, 12.890, and 13.330 eV, respectively. These values are tabulated together with the corresponding VIE values obtained from the simulated spectra in Table VI. The AIEs to the triplet states obtained in this way are very similar to those obtained above, by considering the comparison between the simulated and observed vibrational structure of individual ionizations to the triplet states. For the $^3A_2$ ionization, the difference is only 0.01 eV.

E. Photoabsorption spectrum, Rydberg series, and quantum defects

With our revised assignments and AIE positions of the five cationic states contributing to the second band of the PE spectrum of ClO_2, the Rydberg series converging to these ionization limits observed in the photoabsorption spectrum of ClO_2 reported by Flesch *et al.*[4] have been reanalyzed. Briefly, the origins of the Rydberg series given by Flesch *et al.* were assumed to be correct and their positions were used to calculate the revised quantum defects (δ), employing our new AIE values as the respective ionization limits. The normal selection rules for electronic transitions have applied. Rydberg series converging to the two singlet cationic states have not been considered, as the uncertainties associated with their AIE positions are relatively large, when compared with those of the three triplet states contributing to the second band of the PE spectrum. The results are summarized in Table VII and it can be seen that the revised quantum defects are as expected for chlorine atom Rydberg states.

The major differences between the original assignments by Flesch *et al.* and our present revised assignments are summarized as following. First, the Rydberg series converging to the $^1B_1$ ionic state, with the ionization limit at 12.445 eV, given by Flesch *et al.*, have now been assigned to excitation of the ν_2 bending modes of the $4s$ and/or $4p$ series leading to the ionization limits of the $^3B_2$ and $^3B_1$ cationic states. This revision is based on the revised assignment of the AIE/VIE position of the $^1B_1$ state in the PE spectrum. It is clear from our spectral simulations that the assignment of the AIE position of the ClO_2^+ $^1B_1 \leftarrow ClO_2$ $\tilde{X}\,^2B_1$ ionization to 12.445 eV is incorrect (see the previous discussion on the reassignments of the PE spectrum). In addition, for both the $^3B_2$ and $^3B_1$ states, both the symmetric stretching and bending modes were observed in the simulated and observed PE spectrum (Fig. 3). Second, the revised assignments, as shown in Table VII, suggest that most of the Rydberg series converging to all three triplet states would overlap. It seems inappropriate

to assign the observed photoabsorption features to only one Rydberg series, as Flesch *et al.* did. Finally, with the overlapping Rydberg series and the different vibrational structures of the three cationic triplet state PE bands (particularly for the $^3A_2$ state, where the Franck–Condon overlap gives weak AIE components), it is possible that the origins identified by Flesch *et al*. may not be the origins of the Rydberg series. This would be particularly true for Rydberg series converging to the $^3A_2$ state, if the vibrational structure in the absorption spectrum of the Rydberg state resembles that of the PE spectrum of the corresponding cationic state. In this connection, the quantum defects given in Table VII for the $^3A_2$ state would then be the lower limits.

IV. CONCLUDING REMARKS

In summary, in this work anharmonicity has been incorporated into an existing harmonic FC method, which includes Duschinsky rotation, in a simple fashion, via multidimensional, *ab initio* anharmonic PEFs. Anharmonic vibrational wave functions have been expressed in terms of linear combinations of the products of harmonic oscillator functions. This anharmonic FC model, employing Watson's Hamiltonian, has been conveniently incorporated into our existing harmonic FC code, so that both anharmonicity and the Duschinsky effect can be accounted for in the anharmonic FCF calculations. In general, it was concluded that, from the theoretical point of view, the anharmonic FC method is expected to give more reliable spectral simulations than the harmonic FC method.

Although the disadvantage of Watson's Hamiltonian lies in its different forms for linear and nonlinear molecules, the nonlinear form of Watson's Hamiltonian has been incorporated into the anharmonic treatment, and the incorporation of the linear form of Watson's Hamiltonian into the anharmonic method is underway. For high vibrational states and/or systems, where both the linear and nonlinear configurations may be involved in an electronic transition, further research will be required. However, this is not a problem in the present study on the He I PE spectrum of ClO_2, where all the electronic states studied are nonlinear, with bending angles far from linearity and have apparently deep bending well depths.

As the first test of the proposed anharmonic FCF algorithm, both the harmonic and anharmonic FCF methods were applied to study the first and third bands in the He I PE spectrum of ClO_2. These two PE bands of ClO_2 have rather simple and well-resolved vibrational structures. Comparing the simulated and observed PE spectra, it is clear that the anharmonic FCF method is superior to the harmonic method, because, for example in the first band, the harmonic FC simulation cannot give an overall match with the observed spectrum even after applying the IFCA procedure. This is because the anharmonic effect is important even at low vibrational levels, as shown from the computed expansion coefficients of the anharmonic vibrational wave functions.

The IFCA procedure was applied with the anharmonic FC code to refine the published MRCI geometry of the $\tilde{X}\,^1A_1$ state of ClO_2^+. The first experimentally derived geometry obtained for this cationic state is $R(\mathrm{Cl–O})=1.414\pm0.002$ Å and $\angle\mathrm{O–Cl–O}=121.8\pm0.1°$ and this should be the most reliable one to date. Although the agreement of the harmonic FC simulated spectrum with the observed spectrum is not as good as that of the anharmonic one, the IFCA geometrical parameters of the $\tilde{X}\,^1A_1$ state of ClO_2^+ obtained with harmonic FCF calculations are very close to those with the anharmonic calculations. In this connection, and in view of the different computational resources required for the harmonic and anharmonic FC calculations, the harmonic FCF code can still be considered useful in obtaining experimentally derived geometrical parameters. However, in carrying out the IFCA procedure with the harmonic code, care should be taken in the comparison between the simulated and observed spectra (see Ref. 1). It should also be mentioned that the *ab initio* calculations, required for the harmonic and anharmonic FC calculations, are very different. For the latter, multidimensional PEFs, obtained from energy surface scans, are required. These scans are expected to be considerably more expensive than geometry optimization and harmonic frequency calculations at the minimum-energy geometry, which are required for the harmonic FC code. Nevertheless, energy surface scans do not require a correlation method with analytical energy derivatives (first and/or second). This allows the use of MRCI-type methods, which can deal with excited states and/or states, which cannot be described correctly by a single determinantal wave function, such as an open-shell singlet state. Summarizing, there are different theoretical and practical advantages and disadvantages associated with the harmonic and anharmonic FC methods and the method chosen will depend on the problem under consideration, the quality of the experimental information, and the available computational resources.

The second band in the ClO_2 He I PE spectrum revealed complicated vibrational structure because it involves ionizations to five low-lying electronic states of the cation. The spectral simulations reported here clearly support the MRCI assignments of Peterson and Werner.[5] The simulated spectrum of the second band has reproduced the main vibrational features of the experimental spectrum. However, a perfect match has not been obtained, even with the variations of the AIEs and the relative photoionization cross sections of the ionizations to the five cationic states. A better match may be obtained if the IFCA procedure were carried out for each of the five ionizations. However, this has not been carried out, because well-resolved vibrational structures in the observed spectrum are required for doing this, but this is not available from the observed spectrum. Nevertheless, with the spectral simulations reported here, the ordering of the $^3B_2$, $^3A_2$, $^3B_1$, $^1A_2$, and $^1B_1$ ionic states in the second PE band of ClO_2 seems clear and their AIEs were determined. The usefulness of the powerful combination of high-level *ab initio* calculation and FC analysis in the interpretation of a seriously overlapping spectrum has been clearly demonstrated. In the case of the He I PE spectrum of ClO_2, the combination of MRCI PEFs and the anharmonic FC code has been shown to work well.

ACKNOWLEDGMENTS

The authors are grateful to the Research Grant Council (RGC) of the Hong Kong Special Administrative Region (Project Nos. POLYU 5156/98P, POLYU 5180/99P, and POLYU 5187/00P), and the financial support from the ''Research Center for Modern Chinese Medicine'' (RCMCM) project (Grant No. 9687) funded by the Budget and Resource Committee of the Hong Kong Polytechnic University. D.K.W.M. and E.P.F.L. are grateful for the financial support from The Hong Kong Polytechnic University (Grant No. G-YY066). Support from the EPSRC and Leverhulme Trust is also acknowledged.

[1] F. T. Chau, J. M. Dyke, E. P. F. Lee, and D. C. Wang, J. Electron Spectrosc. Relat. Phenom. **97**, 33 (1998).
[2] J. K. G. Watson, Mol. Phys. **15**, 479 (1968).
[3] F. Duschinsky, Acta Physicochim. URSS **7**, 55 (1937).
[4] R. Flesch, E. Rühl, K. Hottmann, and H. Baumgärtel, J. Phys. Chem. **97**, 837 (1993).
[5] K. A. Peterson and H.-J. Werner, J. Chem. Phys. **99**, 302 (1993).
[6] K. A. Peterson and H.-J. Werner, J. Chem. Phys. **105**, 9823 (1996).
[7] S. Carter and N. C. Handy, Comput. Phys. Rep. **5**, 115 (1986).
[8] D. J. Searles and E. I. von Nagy-Felsobuki, *Ab Initio Calculations of Vibrational Band Origins*, edited by J. R. Durig (Elsevier, New York, 1991), Vol. 19, Chap. 4, pp. 151–213.
[9] J. K. G. Watson, Mol. Phys. **19**, 465 (1970).
[10] G. D. Carney and R. N. Porter, J. Chem. Phys. **65**, 3547 (1976).
[11] R. J. Whitehead and N. C. Handy, J. Mol. Spectrosc. **59**, 459 (1976).
[12] S. Carter and N. C. Handy, Mol. Phys. **57**, 175 (1986).
[13] P. Jensen, J. Chem. Soc., Faraday Trans. 2 **84**, 1315 (1988).
[14] P. Jensen, J. Mol. Spectrosc. **133**, 438 (1989).
[15] P. Jensen, J. Mol. Spectrosc. **128**, 478 (1988).
[16] J. Tennyson and B. T. Sutcliffe, J. Chem. Phys. **77**, 4061 (1982).
[17] J. Tennyson and B. T. Sutcliffe, J. Mol. Spectrosc. **101**, 71 (1983).
[18] J. Tennyson and B. T. Sutcliffe, J. Chem. Phys. **79**, 43 (1983).
[19] J. M. Bowman, Acc. Chem. Res. **19**, 202 (1986).
[20] A. Roitberg, B. R. Gerber, R. Elber, and M. A. Ratner, Science **268**, 1319 (1995).
[21] T. E. Sharp and H. M. Rosenstock, J. Chem. Phys. **41**, 3453 (1964).
[22] P. Botschwina, B. Schulz, M. Horn, and M. Matuschewski, Chem. Phys. **190**, 345 (1995).
[23] P. Botschwina, S. Seeger, M. Mladenovic, B. Schulz, M. Horn, S. Schmatz, F. Jörg, and R. Oswald, Int. Rev. Phys. Chem. **14**, 169 (1995).
[24] K. Takeshita, J. Chem. Phys. **86**, 329 (1987).
[25] K. Takeshita and N. Shida, Chem. Phys. **210**, 461 (1996).
[26] P.-Å. Malmqvist and N. Forsberg, Chem. Phys. **228**, 227 (1998).
[27] L. Serrano-Andres, N. Forsberg, and P. A. Malmqvist, J. Chem. Phys. **108**, 7202 (1998).
[28] D. Xie and H. Guo, Chem. Phys. Lett. **307** (1–2), 109 (1999).
[29] G. Barinovs, N. Markovic, and G. Nyman, J. Chem. Phys. **111**, 6705 (1999).
[30] T. Müller, P. H. Vaccaro, F. Pérez-Bernal, and F. Iachello, J. Chem. Phys. **111**, 5038 (1999).
[31] C. Eckart, Phys. Rev. **47**, 552 (1935).
[32] A. B. Cornford, D. C. Frost, F. G. Herring, and C. A. McDowell, J. Chem. Phys. **55**, 2820 (1971).
[33] A. B. Cornford, D. C. Frost, F. G. Herring, and C. A. McDowell, Faraday Discuss. **54**, 56 (1972).
[34] A. Warshel, J. Chem. Phys. **62**, 214 (1975).
[35] A. Warshel and M. Karplus, Chem. Phys. Lett. **17**, 7 (1972).
[36] A. Warshel and M. Karplus, J. Am. Chem. Soc. **96**, 5677 (1974).
[37] P. Chen, *Photoelectron Spectroscopy of Reactive Intermediates*, edited by C. Y. Ng, T. Baer, and I. Powis (Wiley, New York, 1994), Chap. 8, pp. 371–425.
[38] J. M. Dyke, S. D. Gamblin, N. Hooper, E. P. F. Lee, A. Morris, D. K. W. Mok, and F. T. Chau, J. Chem. Phys. **112**, 6262 (2000).
[39] F. T. Chau, D. C. Wang, E. P. F. Lee, J. M. Dyke, and D. K. W. Mok, J. Phys. Chem. A **103**, 4925 (1999).
[40] E. P. F. Lee, D. C. Wang, and F. T. Chau, J. Phys. Chem. **100**, 19795 (1996).
[41] D. K. W. Mok, E. P. F. Lee, F. T. Chau, and J. M. Dyke, J. Phys. Chem. A (submitted).
[42] M. J. Frisch, G. W. Trucks, H. Bernhard Schlegel *et al.*, GAUSSIAN98 (Gaussian, Inc., Pittsburgh, PA, 1998).
[43] K. A. Peterson, J. Chem. Phys. **109**, 8864 (1998).
[44] T. H. Dunning, Jr., J. Chem. Phys. **90**, 1007 (1989).
[45] D. E. Woon and T. H. Dunning, Jr., J. Chem. Phys. **98**, 1358 (1993).
[46] A. W. Richardson, R. W. Redding, and J. C. D. Brand, J. Mol. Spectrosc. **29**, 93 (1969).
[47] H. S. P. Muller, G. O. Sorenson, M. Birk, and R. R. Friedl, J. Mol. Spectrosc. **186**, 177 (1997).
[48] M. Alcamí, O. Mó, M. Yáñez, and I. L. Cooper, J. Phys. Chem. A **103**, 2793 (1999).
[49] Y. Pak and R. C. Woods, J. Chem. Phys. **104**, 5547 (1996).
[50] E. Ruhl, U. Rockland, H. Baumgartel, O. Losking, M. Binnewies, and H. Willner, Int. J. Mass. Spectrom. **187**, 545 (1999).
[51] U. Rockland, H. Baumgartel, E. Ruhl, O. Losking, H. P. Muller, and H. Willner, Ber. Bunsenges. Phys. Chem. **99**, 969 (1995).